Renewable and Sustainable Energy Reviews 28 (2013) 677–690

Contents lists available at ScienceDirect

Renewable and Sustainable Energy Reviews

journal homepage: www.elsevier.com/locate/rser

A review on the thermodynamic optimisation and modelling of the solar thermal Brayton cycle

W.G. Le Roux [a], T. Bello-Ochende [b,*], J.P. Meyer [a]

[a] Department of Mechanical and Aeronautical Engineering, University of Pretoria, Private Bag X20 Hatfield, Pretoria 0028, South Africa
[b] Department of Mechanical Engineering, University of Cape Town, Private Bag X3, Rondebosch 7701, South Africa

ARTICLE INFO

Article history:
Received 28 April 2013
Received in revised form
31 July 2013
Accepted 11 August 2013
Available online 6 September 2013

Keywords:
Solar
Brayton
Optimisation
Entropy
Modelling

ABSTRACT

Many studies have been published on the performance and optimisation of the Brayton cycle and solar thermal Brayton cycle showing the potential, merits and challenges of this technology. Solar thermal Brayton systems have potential to be used as power plants in many sun-drenched countries. It can be very competitive in terms of efficiency, cost and environmental impact. When designing a system such as a recuperative Brayton cycle there is always a compromise between allowing effective heat transfer and keeping pressure losses in components small. The high temperatures required in especially the receiver of the system present a challenge in terms of irreversibilities due to heat loss. In this paper, the authors recommend the use of the total entropy generation minimisation method. This method can be applied for the modelling of a system and can serve as validation when compared with first-law modelling. The authors review various modelling perspectives required to develop an objective function for solar thermal power optimisation, including modelling of the sun as an exergy source, the Gouy–Stodola theorem and turbine modelling. With recommendations, the authors of this paper wish to clarify and simplify the optimisation and modelling of the solar thermal Brayton cycle for future work. The work is applicable to solar thermal studies in general but focuses on the small-scale recuperated solar thermal Brayton cycle.

Contents

* Corresponding author. Tel.: +27 21 650 3673; fax: +27 21 650 3240.
E-mail addresses: willemleroux@gmail.com (W.G. Le Roux), tunde.bello-ochende@uct.ac.za, tbochende@gmail.com (T. Bello-Ochende), josua.meyer@up.ac.za (J.P. Meyer).

1364-0321/$ - see front matter
http://dx.doi.org/10.1016/j.rser.2013.08.053

Nomenclature

a	constant, –
A	cross-sectional area, m^2
b	constant, –
BSR	blade speed ratio, –
c	constant, –
c	specific heat, J/kg K
COP	coefficient of performance, –
C_s	gas velocity, m/s
d	degradation constant, –
D	turbine diameter, m
e	specific exergy, J/kg
E	exergy, J
f	sunlight dilution factor, –
F_D	external drag force, N
g	gravity constant, m/s^2
h	specific enthalpy, J/kg
I	solar irradiance, W/m^2
J	polar moment of inertia, kg m^2
k	gas constant (c_p/c_v), –
k	thermal conductivity, W/m K
l	thread length, m
L	length, m
m	mass of the rotor assembly, kg
$\dot{m}$	mass flow rate, kg/s
N	speed, rpm
N	number of fins, –
NTU	number of transfer units, –
P, p	pressure, Pa
$\dot{Q}$	heat transfer rate, W
r	pressure ratio, –
r	distance from rotational axis to thread's attachment to the rotor, m
R	gas constant, J/kg K
s	specific entropy, J/kg K
S	solar constant, W/m^2
S	entropy, J/K
$\dot{S}$	entropy rate, W/K
t	time, s
T	temperature, K
T_0	environment temperature, K
U	rotor inlet blade tip speed, m/s
V	velocity, m/s
$\dot{W}$	power, W
x	distance in x-direction, m
y	distance in y-direction, m
z	height, m
z	constant, –
ε	heat exchanger effectiveness, –
η	efficiency, –
κ	dilution factor of diffuse radiation, –
λ	dimensionless parameter for longitudinal conduction, –
σ	Stefan–Boltzmann constant, $W/m^2 K^4$
τ	period time for one oscillation, s
υ	volume, m^3

Subscripts

0	surrounding/loss
0	zero pressure (ideal gas) for c_p
1	at state 1
2	at state 2
1–11	refer to Fig. 1
a	dead (reference) state
acc	acceleration
b	at heat transfer boundary
B	base
BH	Bahnke and Howard
be	beam
c	compressor
col	collector
cv	control volume
d	diffuse
D	destruction
e	exit
eff	effective
eff	efficiency
gen	generation
i	inlet
j	component number
$loss$	loss into the environment
m	mechanical
max	maximum
min	minimum
net	net
opt	optimum
p	for constant pressure
p	planet
r	receiver
reg	recuperator
$rotor$	rotor
R	reversible
s	isentropic
S	Sun
$sngl$	single
t	turbine
v	for constant volume
∞	surrounding area/free stream

Superscripts

*	solar
.	time rate of change
CH	chemical

1. Introduction

Concentrated solar power systems use the concentrated power of the sun, as a heat source in a power cycle, to generate mechanical power. Bejan et al. [1] implied that the solar heat source is more suitable than the isotope and nuclear heat sources when the power plant size is in the range of 2–100 kW. Solar thermal power cycles have potential to be used in many sun-drenched countries. One of these cycles is the solar thermal Brayton cycle. This cycle can be very competitive in terms of efficiency, cost and environmental impact. Chen et al. [2] showed that the Brayton cycle is definitely worth studying when comparing its efficiency with those of other power cycles. Mills [3] predicted that emphasis may shift from Dish–Stirling technology to solarised Brayton micro-turbines due to lower Brayton costs, as a result of high production quantities in the current market. An open solar thermal Brayton cycle uses air as

working fluid, which makes this cycle very attractive for use in water-scarce countries.

In a solar thermal Brayton cycle, a black receiver is usually mounted at the focus of a sun-tracking parabolic dish reflector or mirror field, so that the reflected beam irradiance can be absorbed and converted into heat [4]. A gas is heated directly or indirectly from the concentrated solar radiation and it is then used in the power cycle to power a turbine. A major disadvantage of the solar thermal Brayton cycle is the high receiver operating temperatures required to get reasonable efficiencies. Most Brayton cycles are not self-sustaining at operating temperatures below 480 °C [4]. Narendra et al. [5] noted that to make solar thermal power a real success it is important that extensive work be carried out in the field of receiver materials and their constraints. The material constraints of the solar receiver contribute extensively to exergy loss.

A recuperated solar thermal Brayton cycle allows for lower compressor pressure ratios and higher efficiency. A recuperator (heat exchanger) is used to extract heat from the turbine outlet and transfer it to the cold stream before it is heated in the solar receiver. The highest-efficiency Brayton cycles are recuperative cycles with low compressor pressure ratios. If recuperation is not used, high compressor pressure ratios are required to provide high efficiency [4].

Different configurations of the solar thermal Brayton cycle can be found in the literature. The direct solar thermal Brayton cycle, operating at relatively low pressure, requires a large, hot gas solar receiver due to low gas heat transfer coefficients [6]. An indirect system uses an extra heat exchanger to extract heat from a fluid system in direct contact with the solar radiation at the solar receiver. This configuration allows for smaller solar receivers to be used. In an open Brayton cycle, air as working fluid is free to enter and leave the system. For open Brayton cycles, it is crucial to have natural air movement past the system to prohibit the reinjection of the warm exhaust gas into the system [4]. A radiator is used in a closed Brayton cycle. Helium has been proposed for closed solar Brayton cycles because of its high heat transfer capability and because it is inert.

Heat exchangers can also be used for intercooling and reheating in a solar thermal Brayton cycle. With multi-staging a number of compression and expansion stages are combined in series with coolers and heaters respectively [4]. According to Stine and Harrigan [4], the major advantage of multi-staging is that the cycle can have the high efficiency associated with a recuperated low-pressure ratio cycle, without having the extremely large recuperator as required for a single-stage cycle of the same power output. Maximum efficiency is achieved when equal pressure ratios are maintained across each compressor and each turbine stage. The Ericsson cycle has the potential of attaining Carnot efficiency when a recuperator is used [4]. Thus, the simplest form a solar thermal Brayton cycle is an open system consisting of a compressor, turbine and solar receiver. More complex forms of this cycle can include one or more recuperators, intercoolers, reheaters, radiators, indirect receiver cycles or all these.

According to Stine and Harrigan [4], there are three major losses in actual Brayton cycle engines: duct pressure losses, turbomachine efficiencies and recuperator effectiveness. In the solar thermal Brayton cycle major heat losses also occur at the receiver, recuperator and air exhaust or radiator. No matter what specific configuration of the solar thermal Brayton cycle, the influencing factors to the performance thereof translate mostly into the irreversibilities of the system, which can be minimised. Many studies have been published on individual components used in a typical solar thermal Brayton cycle and their optimisation, although, often these components are optimised individually and not as a part of a whole system with system performance as objective function. In this paper, new perspectives on the optimisation and modelling of the solar thermal Brayton cycle in terms of the second law of thermodynamics are given, conflicts in the literature are shown and recommendations for future work are given.

2. Optimisation of the solar thermal Brayton cycle

2.1. The second law of thermodynamics

Eq. (1) shows an exergy balance for a control volume [1,7]. The definitions for specific exergy transfers at inlets and outlets are given in Eq. (2) [1]

$$\frac{dE_{cv}}{dt} = \sum_j \left(1-\frac{T_0}{T_j}\right)\dot{Q}_j - \left(\dot{W}_{cv} - p_0\frac{dv_{cv}}{dt}\right) + \sum_i \dot{m}_i e_i - \sum_e \dot{m}_e e_e - \dot{E}_D \quad (1)$$

$$e = (h-h_0) - T_0(s-s_0) + 1/2V^2 + gz + e^{CH} \quad (2)$$

There is a fundamental difference between energy and exergy: exergy, unlike energy, uses the environment as its reference point. The exergetic approach is useful, since one would like to know what the optimal possibilities are for us as inhabitants of this environment instead of inhabitants of infinite space.

Entropy generation is a path dependant property and should not be confused with the thermodynamic property entropy change (S_2-S_1) [1]. Eq. (3) [7] gives the expression for the balance of entropy for a control volume

$$\frac{dS_{cv}}{dt} = \sum \dot{m}_i s_i - \sum \dot{m}_e s_e + \sum \frac{\dot{Q}_{cv}}{T} + \dot{S}_{gen} \quad (3)$$

Consider the design of lifting a weight with a pulley system: entropy generation is proportional to additional work wasted for a bad pulley system design [8]. Entropy generation can be minimised. For the entropy change of an ideal gas, Eq. (4) [7] can be used with constant specific heat

$$s_2 - s_1 = c_{p0} \ln \frac{T_2}{T_1} - R \ln \frac{P_2}{P_1} \quad (4)$$

2.2. Exergy analysis

Exergy analysis is often applied to measure the performance of a solar system. Izquierdo et al. [9] for example, studied the entropy generated, the exergy destroyed and the exergetic efficiency of lithium–bromide absorption thermal compressors driven by solar thermal collector heat. Total entropy generation rate for the system was found by summing the entropy generation rates from various entropy generation mechanisms in the system. Narendra et al. [5] presented an exergetic analysis of a solar thermal power system using the Rankine cycle. This analysis was done for the whole system to show the irreversibilities at each part of the system. The collector–receiver assembly was found to be the part with the highest losses. Barrett and Reid [10] showed that the compressor and recuperator are the main contributors to the total entropy generation rate in a 100 kWe Closed-Brayton-Cycle Space Power System optimised for minimum mass. Jubeh [11] did an exergy analysis for an open regenerative Brayton cycle with isothermal heat addition and an isentropic compressor and turbine. The effect of two heat additions in a gas turbine engine, rather than one, was analysed from the view point of the second law of thermodynamics. It was found that the effect of isothermal heat addition on the performance of a recuperated Brayton cycle is positive for low compressor pressure ratios, low ambient temperatures, and high turbine inlet temperatures. Jubeh [11] emphasised that first- and second-law analyses together are crucial for

understanding and explaining the effect of any parameter on the performance of a thermal system.

2.3. Entropy generation minimisation

Thermodynamic optimisation or entropy generation minimisation (EGM) can be applied in an exergy analysis to optimise the performance of a system. To maximise the power output of a power plant is equivalent to minimising the total entropy generation rate associated with the power plant [12,13,14–16]. According to Bejan [12], to minimise the irreversibility of a proposed configuration, the analyst must understand the relationship between temperature differences and heat transfer rates, and between pressure differences and mass flow rates. The entropy generation rate or thermodynamic non-ideality of the design, $\dot{S}_{gen}$, must be described in terms of the topology and physical characteristics of the system, such as dimensions, speeds, shapes and materials [12].

According to Bejan [17], EGM experienced astounding growth during the 1980s and 1990s in both engineering and physics fields. The EGM method relies on the simultaneous application of heat transfer and engineering thermodynamics. It account for the inherent irreversibility due to heat, mass and fluid flow processes of devices and installations [17].

EGM has been applied in various fields. The first power generation field to use EGM simulations regularly was that of solar power plants. It was found that an optimum coupling between a solar receiver and power cycle exists, so that the power output is a maximum [17]. Shiba and Bejan [18] optimised a counterflow heat exchanger that served as a condenser in a vapour-compression-cycle refrigeration system for environmental control of aircrafts. It was shown that the minimisation of the total power requirement was completely equivalent to the minimisation of the entropy generation rate in the entire system. According to Torres-Reyes et al. [19] thermodynamic optimisation (or EGM) can be applied to the thermal design of solar heating systems. In their paper, the architecture of a solar collector with a specific geometry and specific arrangement between the absorber surface and the fluid duct was determined based on global optimisation. Using the theory of entropy generation minimisation, Chen et al. [20] optimised the internal and external irreversible closed recuperative Brayton heat pump cycle coupled to constant and variable temperature heat reservoirs. They found that there exists an optimum matching between the effectivenesses of the hot side and cold side heat exchangers of the system and the regenerator and that for maximum *COP* of the heat pump, an optimum pressure ratio exists. Zheng et al. [21] established an irreversible cycle model of a solar-driven Braysson heat engine (a hybrid power cycle based on the conventional Brayton cycle). They found that for maximum efficiency, there is an optimum value of the solar collector operating temperature for a given set of operating parameters. Wu et al. [22] also presented such a system in which the temperature dependent heat capacity of the working fluid, the radiation–convection heat losses from the solar collector and the irreversibilities due to heat transfer and non-isentropic compression and expansion processes were taken into account. They found that the overall maximum efficiency and optimum operating temperature of the collector decrease as the heat losses of the collector increases.

According to Salamon et al. [23], minimising the rate of entropy generation and maximising the power both push an operation toward minimum wastefulness, while minimum entropy generation and maximum power output are opposite when considering frugality. Therefore, minimum entropy generation is considered as the objective of the conservationist and maximum power as the objective of the industrialist when for example, managing an existing power plant or driving a motor vehicle [23]. In this paper, however, the term entropy generation minimisation refers rather, to the optimisation of geometries of a specific design such that a system performs optimally. For example, the geometries of the power producing parts of the engine of a motor vehicle can be designed in such a way that it produces maximum power output when a specific amount of fuel is available.

2.4. Optimisation results and influencing factors

The Brayton cycle and its optimisation have often been investigated in the literature. Chen et al. [24] gave the power output and the efficiency of a regenerative and closed Brayton cycle as functions of pressure ratios, reservoir temperatures, heat exchanger effectiveness, compressor and turbine efficiencies, and working fluid thermal capacitance rates. They found that the maximum power output of the system is strongly dependant on the effectiveness of the recuperator and that the maximum power output is attained when the system hot and cold side effectivenesses are arranged in a particular way. Wu et al. [25] studied the performance of an endoreversible regenerative Brayton heat engine with focus on minimising irreversibilities at the hot and cold side heat exchangers of the system (for example, the solar receiver and the radiator) and the recuperator. They found maximum net power output of the system when the hot and cold side heat exchangers and the recuperator are ideal. However, these conditions require infinitely large components, making the system impractical.

Stevens et al. [26] and Stevens and Baelmans [27] stated that a recuperator is often used to improve the overall cycle efficiency of a standard gas turbine and that a high heat exchanger effectiveness and low pressure drop are required to achieve maximum cycle efficiency. According to these authors, finding a compromise between these conflicting requirements is the main challenge in recuperator design. Stevens and Baelmans [27] found that for maximum cycle efficiency, the cold and hot side pressure drops of a micro-recuperator used in a gas turbine cycle are uniquely connected, since their ratio depends primarily on the compressor pressure ratio. Stevens et al. [26] also found that the recuperator effectiveness should be as high as possible and that the pressure drop should be preferably located at the cold side of the recuperator. Thus they concluded that the hot channels should be larger than the cold channels. They also concluded that for a fixed recuperator volume optimisation, the recuperator should be as short as possible with as high as possible cross-sectional area.

By comparing and considering three different gases, Riazi and Ahmed [28] presented an analysis on the effect of the ratio of specific heats (k) of a closed regenerative solar Brayton cycle. They found that a fluid with a high ratio of specific heats, for example air ($k=1.4$), has peak efficiencies at lower compressor pressure ratios while a fluid with a low ratio of specific heats, for example CF_4 ($k=1.14$), has peak efficiencies at higher compressor pressure ratios. Also, a fluid with a high ratio of specific heats performs well when the temperature ratio (ratio between highest and lowest temperature in cycle) is also high, while it performs poor when the temperature ratio is low. In comparison with air, a fluid with a low ratio of specific heats performs better at low temperature ratios.

Roco et al. [29] presented a general theoretical framework for a recuperative gas turbine cycle with external and internal irreversibilities, in order to study the maximum power output, maximum efficiency, efficiency at maximum power, power at maximum efficiency, and optimum pressure ratios. The optimal operating conditions were investigated in terms of the isentropic efficiencies of the compressor and turbine, pressure drops in the hot and cold streams, and effectiveness of the heat exchangers. They found that the maximum efficiency and maximum power operating points are coincident at a recuperator efficiency of 50%.

Cheng and Chen [30] used thermodynamic optimisation to optimise the power output of an endoreversible intercooled Brayton cycle coupled to two heat reservoirs with infinite thermal capacitance rates. The effects of intercooling on the maximum power of an endoreversible Brayton cycle were examined. They found that an endoreversible intercooled Brayton cycle is better than an endoreversible simple Brayton cycle without lowering the thermal efficiency. A similar work was also done by Wang et al. [31]. They found that there exists an optimal intercooling pressure ratio for maximum power.

Zhang et al. [32] established a model in which the heat losses of the solar collector and the external and internal irreversibilities of a solar-driven Brayton heat engine were taken into account. Thus, this model was done for a solar thermal Brayton cycle without a recuperator. It was found that the performance characteristics of an irreversible solar thermal Brayton heat engine are different from those of a solar-driven heat engine consisting of an endoreversible Brayton heat engine. It was found that the larger the heat losses in the solar collector, the lower the optimum operating temperature of the solar collector and the smaller the maximum overall efficiency of the system.

2.5. Optimisation of the solar thermal Brayton cycle using EGM and geometry optimisation

In most of the abovementioned analyses using EGM (or minimisation of irreversibilities), however, geometry optimisation was not done (except for example [26]). The effects of component geometries were thus not included. The many influencing factors to the performance of the system can be much better understood with the use of entropy generation minimisation and the optimisation of geometries for each unique case of the solar thermal Brayton cycle.

Geometric optimisations for the solar thermal Brayton cycle were done by Le Roux et al. [33–35]. Le Roux et al. [33] found that the optimised systems' irreversibilities were spread throughout the system in such a way that the internal irreversibility rate was almost three times the external irreversibility rate. The geometries of a modified cavity receiver and plate-type recuperator in an open and direct solar thermal Brayton cycle were optimised using EGM and is shown in the following example.

When taking a control volume around an open and direct solar thermal Brayton system and assuming a steady state, it can be determined where exergy is crossing the boundary. This is shown in Fig. 1 [33–35]. An exergy analysis was performed for the system. Take note that the inlet and outlet temperatures of the system are not the same, but the pressures are. Also note that $T_{10}=T_{11}$ as it is assumed that the control volume boundary is very close to the hot

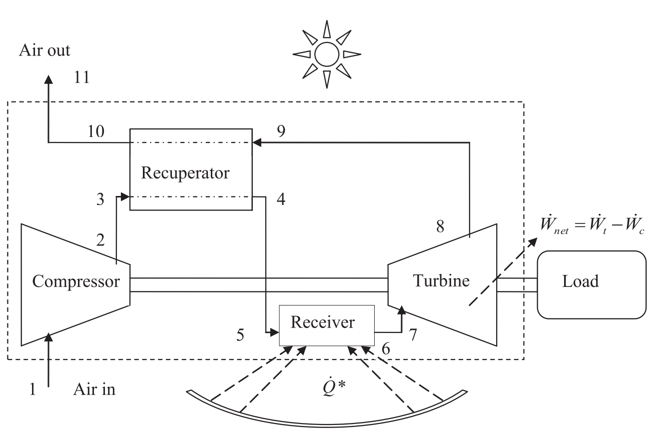


Fig. 1. Control volume around the open and direct solar thermal Brayton cycle to perform an exergy analysis [33–35].

stream exit of the recuperator. The following equations arise which can be used as objective functions [33–35]:

$$T_0\dot{S}_{gen}=\dot{m}e_i-\dot{m}e_e+\left(1-\frac{T_0}{T^*}\right)\dot{Q}-\left(1-\frac{T_0}{T_{b,j}}\right)\dot{Q}_{loss,j}-\dot{W}_t+\dot{W}_c$$

$$\therefore\quad T_0\dot{S}_{gen}=\dot{m}\left[h_i-h_e-T_0(s_i-s_e)+\tfrac{1}{2}(V_i^2-V_e^2)+g(z_i-z_e)\right]+\left(1-\frac{T_0}{T^*}\right)\dot{Q}^*-\left(1-\frac{T_0}{T_{b,j}}\right)\dot{Q}_{loss,j}-\dot{W}_{net} \quad (5)$$

or

$$\dot{W}_{net}=\dot{W}_t-\dot{W}_c=-T_0\dot{S}_{gen}+\frac{\dot{m}}{2}(V_i^2-V_e^2)+\dot{m}g(z_i-z_e)+\left(1-\frac{T_0}{T^*}\right)\dot{Q}^*-\left(1-\frac{T_0}{T_{b,j}}\right)\dot{Q}_{loss,j}+\dot{m}c_{p0}(T_1-T_{11})-\dot{m}T_0c_{p0}\ln\left(\frac{T_1}{T_{11}}\right) \quad (6)$$

Furthermore, the total internal entropy generation rate of the system can be written in terms of the sum of the entropy generation rate of each component and duct in the system. The entropy generation rate of each component is in turn a function of geometry variables. Thus, we have the total internal entropy generation rate as [33–35]

$$\dot{S}_{gen}=\sum\dot{S}_{gen,j}=\dot{S}_{gen(compressor)}+\dot{S}_{gen(duct23)}+\dot{S}_{gen(recuperator)}+\dot{S}_{gen(duct45)}+\dot{S}_{gen(receiver)}+\dot{S}_{gen(duct67)}+\dot{S}_{gen(turbine)}+\dot{S}_{gen(duct89)}+\dot{S}_{gen(other)} \quad (7)$$

Eq. (7) can then be substituted into Eq. (6) to get the net power output for the open and direct solar thermal Brayton cycle. The net power output is then written in terms of the total entropy generation rate of each of the components and ducts in the system. Note the cancelation of the terms $(T_0/T_{b,j})\dot{Q}_{loss,j}$ and $(T_0/T^*)\dot{Q}^*$ in the objective function when the entropy generation terms from Section 3 are added into Eqs. (5)–(7). This equation can then be written in terms of all the geometry variables in the system. This equation for the net power output is the objective function, which should be maximised by optimising the geometry variables that describe the temperatures and pressures at each point in the system, subject to global constraints. The components of Eq. (7) are discussed in Section 3.

Eq. (6) is also found in a similar form in various exergy analyses of existing systems for example by Karsli [36]. A similar approach for a nuclear power plant was taken by Gomez et al. [37] so that the total entropy generation rate was written in terms of the power output of the system. A similar exergy analysis was also done by Jubeh [11]. In these systems, however, exergy analysis was done without optimisation.

In the following section the building blocks for structuring a unique objective function for the optimisation of the component geometries of a specific solar thermal Brayton cycle is given. The many influencing factors to the performance of a specific solar thermal Brayton cycle with unique components can be much better understood with the use of entropy generation minimisation.

3. Structuring the objective function for solar thermal Brayton cycle optimisation

In this section, the importance of modelling different sections in a system so that an objective function can be derived is emphasised. The modelling of these various sections and components are discussed and conflicts and new perspectives are highlighted.

3.1. The Gouy–Stodola theorem

The Gouy–Stodola theorem (Eq. (8)) states that the lost available work (see Eq. (1)) is directly proportional to the entropy

generation in a system [1,8,38]. This theorem allows an analyst to describe a quantity to be maximised, such as the power output of a system, in terms of the total entropy generation rate in a system. The Gouy–Stodola theorem is named after Gouy (1889) and Stodola (1910) who recognised its importance. The Gouy–Stodola theorem has been applied and referred to in various solar thermal studies including for example Cervantes and Torres-Reyes [39], Amhalhel and Furmański [40], Sieniutycz and Kuran [41] and Hepbasli [42]

$$\dot{E}_D = T_0 \dot{S}_{gen} \tag{8}$$

According to Lampinen and Wikstén [43], in all previous studies, as well as in the theories given by Bejan [44] and by Tolman and Fine [45], a general method of finding the correct temperature to be used as a proportionality factor for the entropy generation rate in the calculation of the power loss, Eq. (8), has remained an open question. Lampinen and Wikstén [43] presented a solution to the classical problem of how to determine the correct temperature. They explained that according to Holmberg et al. [46], if the system only exchanges heat at the environmental temperature, the Gouy–Stodola theorem gives the correct loss of power. Most industrial processes, however, exchange heat at higher or lower temperatures than the environmental temperature [46]. If the environmental temperature is then used to calculate the loss of power in these cases, the Gouy–Stodola theorem does not give the correct loss [46]. According to Holmberg et al. [46], using the theory of Lampinen and Wikstén [43]

$$\dot{E}_D = \dot{W}_{net,R} - \dot{W}_{net} = T_{eff} \dot{S}_{gen} \tag{9}$$

where

$$T_{eff} = \frac{h_2 - h_{2R}}{s_2 - s_{2R}} \tag{10}$$

Or, if the specific heat capacity and pressure remain constant

$$T_{eff} = \frac{T_2 - T_{2R}}{\ln(T_2/T_{2R})} \tag{11}$$

where, for a system, h_2 is the specific enthalpy of the flow at the outlet and s_2 is the specific entropy at the outlet and where h_{2R} and s_{2R} represent states of the enthalpy and entropy after a reversible process, respectively.

According to Bejan [12], it is important to stress that T_0 in Eq. (8) is the temperature of those areas of the environment that are adequately close to the system but which are not affected by the discharge of the system. According to Bejan [12], the purpose of such a modelling decision is to place all the internal and external irreversibilities related to the physical installation inside the system. The system then consists of the installation and the surrounding areas which are affected by the installation. In an actual system, rejected heat would leave the installation and enter the bordering environmental fluid at a temperature higher than T_0. The same heat would also cross the T_0 boundary further down the line [12].

Thus, the authors of this paper emphasise that the choice of the control volume boundary is very important in the thermodynamic analysis of the solar thermal Brayton cycle. The authors recommend that for a system, Eq. (8) be used. Note that the heat losses from components should then be calculated as the heat loss up to the temperature, T_0. When calculating lost available work for a single component, Eqs. (10) and (11) can be used to calculate the boundary temperature, T_j as shown in Eqs. (5) and (6).

3.2. The sun as an exergy source

The solar input for the solar thermal Brayton cycle can be modelled in different ways in an objective function such as Eqs. (5) and (6). The following literature gives a review thereof, by highlighting conflicts and new perspectives.

According to Izquierdo Millan et al. [47], before solar radiation can be converted into mechanical power, it is first converted into heat when it is intercepted by an absorbent surface located on the Earth. This occurs with a great loss of exergy. The exact exergy of solar radiation could be determined with spectral measurement and calculation according to Petela [48]. The concept of solar exergy maps has also been developed by Joshi et al. [49].

According to Onyegegbu and Morhenne [50], the expressions for radiation temperature and exergy of direct beam solar radiation are well documented. The expression for exergy of solar radiation and the history of its development have also been investigated and documented more recently by various authors [42,51–56]. Throughout the literature [57–60] the absorbed solar radiation exergy rate, considering the Petela theorem [61], is given by

$$\dot{E} = \dot{Q}^* \left(1 - \frac{4}{3}\left(\frac{T_a}{T_s}\right) + \frac{1}{3}\left(\frac{T_a}{T_s}\right)^4\right) \tag{12}$$

where T_s is the apparent blackbody temperature of the sun and $\dot{Q}^*$ is the total solar power input crossing a control volume boundary. According to Eskin [62], the expression for the availability of solar radiation (W/m^2) with beam and diffuse components as given by Onyegegbu and Morhenne [50] is

$$\dot{E} = I_{be}\left(1 - \frac{4}{3}\left(\frac{T_a}{T_s}\right)\right) + I_d\left(1 - \frac{4}{3}\left(\frac{T_a}{T_s^*}\right)\right) \tag{13}$$

where

$$\frac{T_s}{T_s^*} = 0.9562 + 0.2777\ \ln(1/\kappa) + 0.0511\kappa \tag{14}$$

The expression for T_s/T_s^*, relating the effective temperature of diffuse radiation to the solar temperature, is obtained from Landsberg and Tonge [63], with κ, the dilution factor of diffuse radiation, less than 0.1.

According to Bejan [8], when doing an exergy analysis on a solar thermal system, the sun can be considered as an exergy-rich source and as a high-temperature fuel. Bejan [44] showed that the exergy rate of the sun is given as

$$\dot{E} = \dot{Q}^* \left(1 - \frac{T_0}{T^*}\right) \tag{15}$$

where T^* is the apparent sun's temperature as an exergy source and $\dot{Q}^*$ is the solar heat rate crossing a control volume boundary. This method has been adopted for the exergy inflow of solar collectors by various authors [13, 33–36, 42, 64, 65]. Eq. (15) has also been used to describe the exergy inflow for heliostat surfaces [66,67]. The abovementioned authors mostly adopted the value T^*, as suggested by Petela [61], being approximately equal to $0.75T_s$ [68,69] (see Eq. (12)). T_s is the apparent blackbody temperature of the sun, which is about 6000 K, or 5762 K [47, 70]. Therefore, T^* is considered to be close to 4500 K [68, 69].

Farahat et al. [58] claimed that according to Najian [71], Eq. (12) violates the second law of thermodynamics and that the corrected equation according to Torres-Reyes et al. [72] and Najian [71], assuming the sun as an infinite thermal source, is Eq. (16), with T^* as the apparent sun temperature and equal to 75% of blackbody temperature of the sun (4350 K) [68]. Also note the inclusion of an optical efficiency, η

$$\dot{E} = \eta I \left(1 - \frac{T_0}{T^*}\right) \tag{16}$$

According to Onyegegbu and Morhenne [50], the expression for the exergy flux which has the widest acceptability is the expression

$$\dot{E} = \dot{Q}^* \left(1 - \frac{4}{3}\left(\frac{T_a}{T_s}\right)\right) \tag{17}$$

The selection of the control volume around the analysed system and the selection of $\dot{Q}^*$, or the term in front of the bracket in Eqs. (12) and (15)–(17), are very important. $\dot{Q}^*$ depends on which boundary is referred to in the analysis. For example, Eqs. (12) and (15)–(17) can be used to describe the incoming exergy from the sun or the incoming exergy from a reflector, see Fig. 2. $\dot{Q}^*$ can thus be the beam irradiance, in the case where it is coming from a reflector for example (hence the inclusion of the optical efficiency in Eq. (16)), or $\dot{Q}^*$ can be the global solar radiation with a boundary somewhere in the atmosphere or even in space. For example, Xu et al. [67] described $\dot{Q}^*$ as the incident solar radiation so that $\dot{Q}^*$ is defined as IA where I is the amount of solar radiation received per unit area, which is the direct normal irradiation (DNI). The available solar radiation per unit area from the sun varies throughout days, months and environmental conditions. The best database for solar irradiance would be the long-term measured data at the site of the proposed solar system [73]. A meteorological database can also be used [74].

According to [47, 70, 75, 76], the global irradiance or the extraterrestrial solar radiation normal to the unit area is the solar constant and is described by

$$S = f\sigma T_s^4 \quad (\mathrm{W/m^2}) \tag{18}$$

where f is the sunlight dilution factor, equal to 2.16×10^{-5} on the earth, σ is the Stefan–Boltzmann constant (5.67×10^{-8} W/m^2 K^4), and T_s is the temperature of the sun (K). According to De Vos [77], cited by [42,47,78], solar exergy can be defined as

$$\dot{E} = f\sigma T_s^4 - (1-f)\sigma T_p{}^4 \tag{19}$$

where $(1-f)\sigma T_p$ is the albedo of the earth, and T_p is the planet temperature. The term, $\sigma T_{col}{}^4$, can also be subtracted from Eq. (19) to include the loss of exergy due to the temperature of the collector.

According to [42, 70, 75], Winter et al. [79] regard the exergy released by solar irradiance as

$$\dot{E} = f\sigma T_s{}^4 \left(1 - \frac{4}{3}\left(\frac{T_a}{T_s}\right)(1 - 0.28 \ln f)\right) \tag{20}$$

Table 1 compares the methods described in the above literature to calculate the solar exergy rate. It is assumed that $\dot{Q}^*$ is equal to $I = 1000$ W/m^2, $\eta = 0.85$, $T^* = T_s = 5777$ K and $T_p = 300$ K. Note that Eqs. (12) and (15) give the same result for all practical reasons.

It is recommended by the authors that Eq. (16) be used in the analysis of the solar thermal Brayton cycle with T^* as the apparent sun temperature and equal to 75% of blackbody temperature of the sun. Also, I is the measured DNI and η is the reflectivity of the reflector. The dish reflector is thus not included in the control volume for analysis.

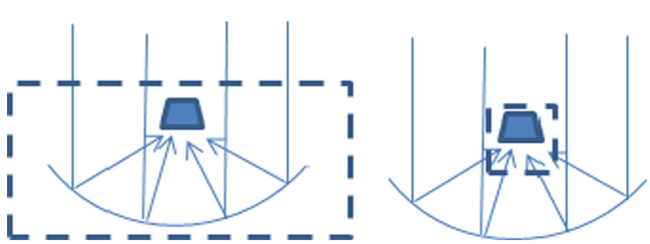


Fig. 2. Control volume boundary including or excluding the solar reflector.

Table 1
Comparison of exergy rate calculated with different methods.

Equation	Solar exergy rate (W/m^2)
(12)	930.76
(15)	930.76
(16)	849.31
(19)	904.84
(20)	985.54

3.3. Modelling of entropy generation mechanisms in the solar thermal Brayton cycle

In a solar thermal power cycle or solar thermal convertor, there will always be entropy generation mechanisms. These mechanisms are mostly due to fluid flow and heat transfer. Bejan [8] provided a number of features most guilty of entropy generation of which those featuring in the solar thermal Brayton cycle are: heat transfer across a non-zero temperature difference, flow with friction, mixing, filling and discharge, compression and expansion. Bejan [38] also presented the entropy generation mechanisms involved with the conversion of solar radiation into mechanical power as adiabatic free expansion, the transformation of monochromatic radiation into blackbody radiation, scattering and net radiative heat transfer.

Bejan et al. [1] considered the simultaneous effect of heat transfer and fluid friction on entropy generation and showed that they have a tendency to contest with one another when a thermodynamic optimum is desired. Entropy generation mechanisms have also been described by Tolman and Fine [45]. In this section, for the different components in the solar thermal Brayton cycle, the entropy generation mechanisms are considered in more detail and recommendations are made on how these entropy generation mechanisms can be put into equation form in an objective function (see Eqs. (5)–(7)).

3.3.1. Solar receiver

According to Bejan [8], there exist three main features that cause irreversibilities in the operation of any solar receiver: heat exchange between the sun and the receiver, heat loss from the receiver to the environment and the internal irreversibility in the receiver. The entropy generation rate from a solar receiver can be written as Eq. (21) [13, 38, 80], where the solar receiver receives solar radiation at the rate, $\dot{Q}^*$

$$\dot{S}_{gen} = \frac{\dot{Q}_0}{T_0} + \frac{\dot{Q}_r}{T_r} - \frac{\dot{Q}^*}{T^*} \tag{21}$$

where T^* is the apparent sun temperature as an exergy source, T_0 is the ambient temperature, and T_r is the surface temperature of the absorber or receiver temperature. For a non-isothermal receiver and neglecting pressure loss [8,13,81]

$$\dot{S}_{gen} = \frac{\dot{Q}_0}{T_0} + \dot{m}c_p \ln\frac{T_{out}}{T_{in}} - \frac{\dot{Q}^*}{T^*} \tag{22}$$

The entropy generation rate in the receiver of an open and direct solar thermal Brayton cycle is given in Eq. (23) for an ideal gas working fluid, where the effect of pressure loss is included. This equation is given by Le Roux et al. [33–35]. Note that $\dot{Q}_0/T_0$ in Eqs. (21)–(23) can be replaced with $\dot{Q}_{loss,receiver}/T_b$ where T_b is the temperature of the boundary across which the heat is being transferred. With this replacement, these equations can be used in Eqs. (5)–(7)

$$\dot{S}_{gen} = -\frac{\dot{Q}^*}{T^*} + \frac{\dot{Q}_0}{T_0} + \dot{m}c_{p0} \ln\left(\frac{T_e}{T_i}\right) - \dot{m}R \ln\left(\frac{P_e}{P_i}\right) \tag{23}$$

From Eq. (23), it is shown that to calculate the entropy generation rate of a solar receiver, the net absorbed heat rate, heat loss rate, and inlet and outlet temperatures and pressures are required. These values will depend on the time of day, month and year as well as the receiver type and receiver design. Computer software and algorithms are available to compute the solar heat rate on a receiver as reflected from a reflector (see for example [82]).

Various solar receivers can be used for the solar thermal Brayton cycle. These include tubular cavity receivers, open or closed volumetric receivers and particle receivers. Bertocchi et al. [83] described the heating of air temperatures to far more than 1000 °C, using a high-temperature solar particle receiver. Kim et al. [84] and Miller and Koenigsdorff [85] also described the features and modelling of a particle receiver. Kim et al. [84] found many experimental results including an increase in the opacity of the particle curtain with mass flow rate up to a constant value near the terminal velocity. Miller and Koenigsdorff [85] found that the main loss from the receiver is reflection from the window, followed by emission and reflection from inside the receiver. Heller et al. [86] demonstrated that pressurised (closed) volumetric receivers are able to produce air of 1000 °C. Pressurised volumetric receivers and its modelling are described in the literature [87–89]. Hischier et al. [87] recommended that a minimisation of the cavity wall thickness in relation with its strength to withstand the operating pressures should be performed. Open volumetric receivers were described by Ávila-Marín [90] and Karni et al. [91]. Karni et al. [91] presented a “Porcupine” volumetric solar receiver and its ability to withstand a solar flux of up to about 4 MW/m^2, while producing gas exits temperatures of up to 940 °C. This receiver consists of an array of pin-fins or elongated heat transfer elements, implanted in a base plate.

The investigation and modelling of tubular cavity receivers are available from the literature [92–94]. The performance of different cavity receivers was investigated by various authors [92,95,96]. Shuai et al. [92] investigated different classical cavity geometries and found that the shape of the cavity (geometry) has a significant effect on the overall distribution of the radiation flux in the cavity receiver. According to Shuai et al. [92], an upside-down pear cavity might be an appropriate shape. Prakash et al. [95] investigated heat losses from a cavity receiver at different inclination angles, with frontal and side winds. Reddy and Sendhil Kumar [96] numerically compared various kinds of cavity receivers and found that their modified cavity receiver experienced lower convection heat losses than other receivers and suggested that their modified cavity receiver may be favoured in a solar dish collector system. For the modified cavity receiver, numerical investigations regarding natural convection heat losses [97,98] and radiation losses [99] were presented for the modified cavity receiver. Le Roux et al. [33–35] described the modelling of a modified solar cavity receiver in detail.

When a dish with a specific diameter, focal length and rim angle is used to focus sun rays onto a receiver, the net rate of heat absorbed by the working fluid in the receiver depends on the aperture diameter of the receiver. Due to the sun's rays not being truly parallel and due to concentrator errors, the reflected rays from the dish form an image of finite size centred on its focal point. The aperture area of the solar receiver will determine the amount of intercepted heat, but also the amount of heat lost due to convection and radiation. The larger the cavity aperture, the more heat can be lost due to convection and radiation but also, the more heat can be intercepted [4]. For a fixed dish concentrator area, the amount of heat available for the working fluid, which is the intercepted heat minus the heat lost due to radiation, convection and conduction, is a function of the cavity aperture diameter.

Steinfeld and Schubnell [94] presented a semi-empirical method to determine the optimum aperture size and operating temperature of a solar cavity receiver for maximum energy conversion efficiency. They found that for inaccurate concentrators, with Gaussian flux density distribution at the focal plane, the optimum operating temperature varies in the range of 800–1300 K. Stine and Harrigan [4] presented a receiver sizing algorithm which can be used with a fixed dish concentrator area to get the intercepted heat for a specific cavity aperture area.

Using the abovementioned literature, the authors recommend that Eq. (23) be geometrised (written in terms of receiver geometry) for a specific solar receiver design with specific constraints, so that geometry variables can be used in an optimisation procedure.

3.3.2. Recuperator or heat exchanger

Heat exchangers play an important role in the solar thermal Brayton cycle as recuperator, intercooler and in indirect systems where the working fluid is not cycled directly through the hot side (receiver). The geometry variables chosen for optimisation in a heat exchanger will depend on the design and type of heat exchanger, since many different types of heat exchangers exist. A recuperator is used in the Brayton cycle to extract the heat from the turbine outlet and transfer it to the cold stream before it is heated by the heat source.

Entropy generation minimisation has been utilised in various heat exchanger applications for optimisation of geometry [18,100,101]. These optimisations were done for components individually and not as part of a whole system. Lerou et al. [101] showed that the width, height and length of flow channels can be optimised by minimising the entropy generation.

According to Bejan [8] and Bejan et al. [1], the irreversibility in a heat exchanger is the sum of the irreversibilities of each of the two surfaces of the heat exchanger. Two factors, temperature difference and frictional pressure drop, are responsible for irreversibilities in heat exchangers [8,102,103]. Yilmaz et al. [103] implied that the greatest source of irreversibility in a heat exchanger comes from fluid friction in the form of pressure drop.

Exergy analysis has been applied on various heat exchanger types. Sarangi and Chowdhury [104] expressed the entropy generation in a counterflow heat exchanger and a nearly ideal heat exchanger. The contribution of fluid friction to the entropy generation was neglected. Adiabatic ends with no heat loss to the surroundings were also assumed for the heat exchanger.

Exergetic optimisation has been done for tubular heat exchangers. Cornelissen and Hirs [105] did an exergetic optimisation of a balanced water-to-water counterflow heat exchanger by considering the irreversibilities due to pressure drop, due to temperature difference between the hot and the cold stream and also due to the production and construction of the heat exchanger. Heat loss to the environment and heat resistance of the tube walls were neglected. Zimparov [106] included the effect of fluid temperature variation along the length of a tubular heat exchanger.

Second law analysis and optimisation were done for heat exchangers with ideal gas flow, as expected in a solar thermal Brayton cycle recuperator. Hesselgreaves [107] considered heat exchangers with zero and finite pressure drop. When looking at zero pressure drop, Hesselgreaves [107] included balanced counterflow, flow imbalance, unbalanced counterflow, parallel flow, condensing on one side and evaporation on one side. Hesselgreaves [107] found that, for zero pressure drop, flow imbalance increases entropy generation and that it is advantageous to let the highest capacity rate stream be the hot stream. Thermodynamic analyses for the balanced cross-flow recuperative plate-type heat exchanger with unmixed fluids were done by Oğulata et al. [102]. Ordóñez and Bejan [108] did a numerical optimisation for the parallel-plate heat exchanger.

The entropy generation rate in the recuperator is shown in Eq. (24) for an ideal gas in the flow channels of the heat exchanger. This equation or a similar version is also used in the literature by various authors [1,8,11,102,103,107,108] and is recommended by the authors of this paper

$$\dot{S}_{gen} = \dot{m}c_{p0}\ln(T_2/T_1) + \dot{m}c_{p0}\ln(T_4/T_3) + \dot{m}c_{p0}\ln\left[(P_2/P_1)^{(1-k)/k}\right] + \dot{m}c_{p0}\ln\left[(P_4/P_3)^{(1-k)/k}\right] + \frac{\dot{Q}_{loss,reg}}{T_b} \tag{24}$$

The fluid going from position 1 to position 2 is the cold stream and the fluid going from position 3 to position 4 is the hot stream in the heat exchanger as shown in Fig. 3.

According to Ordóñez and Bejan [108], entropy is also generated due to the discharge at the recuperator in an open cycle—hence Eq. (25). The equation to be used in an analysis depends on the definition of the boundaries of the control volumes of the recuperator and the system

$$\dot{S}_{gen} = \dot{m}c_{p0}\ln(T_2/T_1) + \dot{m}c_{p0}\ln(T_4/T_3) + \dot{m}c_{p0}\left[\frac{T_2 - T_0}{T_0}\right] + \dot{m}c_{p0}\ln\left[(P_2/P_1)^{(1-k)/k}\right] + \dot{m}c_{p0}\ln\left[(P_4/P_3)^{(1-k)/k}\right] + \frac{\dot{Q}_{loss,reg}}{T_b} \tag{25}$$

Eq. (25) should not be used when the entropy generation due to the exhaust of the open system (warm air outlet) is already added as a separate entropy generation mechanism. The authors recommend that Eq. (24) is used in conjunction with an objective function such as Eqs. (5)–(7).

Different designs are available for the Brayton cycle recuperator. In solar applications, the recuperator is often designed as integral to the micro-turbine. To model the recuperator entropy generation (Eq. (24)), the inlet and outlet temperatures and pressures, and the heat loss from the recuperator are required. The heat loss to the environment from the surface of the recuperator can be a significant factor and it is recommended that it is included in solar thermal Brayton cycle analysis. Hesselgreaves [107], Oğulata et al. [102] and Ordóñez and Bejan [108] suggested that the $\varepsilon - NTU$ (effectiveness – number of transfer units) method, based on the second law of thermodynamics, can be used to get the outlet temperatures and the total heat transfer rate from the hot fluid to the cold fluid. This is shown in the literature by Haugwitz [109] and Le Roux et al. [33–35].

In many counterflow heat exchangers, the heat flow through the material in the longitudinal direction is neglected in determining the temperature profile over the heat exchanger. Eq. (26) ([101]) is a dimensionless parameter that can be used to see if longitudinal conduction can be neglected or not. k is the thermal conductivity of the heat exchanger material and A is the cross-sectional area. The longitudinal conduction cannot be neglected if $\lambda_{BH} > 10^{-2}$ [101]

$$\lambda_{BH} = \frac{kA}{L\dot{m}c_{p,\min}} \tag{26}$$

A few examples of recuperator designs and the modelling thereof are given: heat exchangers are required to be efficient, safe, economical, simple and convenient [103]. Heat transfer and pressure losses as well as the optimisation of price, weight and size should be considered while designing the heat exchanger [102].

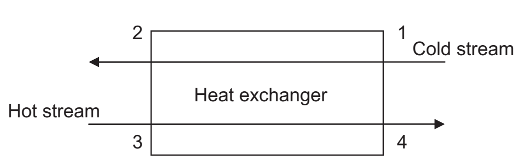


Fig. 3. Heat exchanger with cold stream (1–2) and hot stream (3–4).

According to Bejan [8], heat exchanger irreversibilities can be decreased by slowing down the fluid which is travelling through the heat exchanger. Also, for a fixed-area heat exchanger, the irreversibility can be reduced by allocating the area correctly [8].

Kreith and Kreider [110] and Hesselgreaves [107] suggested that counterflow heat exchangers should be used in solar thermal power systems and that parallel-flow heat exchangers should be avoided. According to Bejan [8], counterflow heat exchangers are often used in recuperative heating associated with the Brayton cycle. It was also suggested by Shah [111] that counterflow plate-type heat exchangers can be used as compact recuperators with micro-turbines. Shah [111] gave design criteria for micro-turbine recuperators. Criteria such as high performance with minimum cost, high exchanger effectiveness, compactness, 40,000 h operation life without maintenance and low pressure loss ($<5\%$) were given. According to Shah [111], these criteria translate into a thin foil primary surface recuperator where flow passages are formed with stamping, folding and welding side edges by an automated operation. Such a recuperator was discussed by McDonald [112,113].

Pra et al. [114] described printed circuit technology and plate fin technology for recuperators while Tsai and Wang [115] investigated the design and analysis of a Swiss–Roll recuperator. Le Roux et al. [33–35] described the modelling of a plate-type recuperator. Traverso and Massardo [116] discussed the furnace-brazed plate-fin type and the welded primary surface type recuperators. Ultiainen and Sundén [117] reviewed a recuperator with cross corrugated or chevron pattern heat transfer surface. Different recuperator designs [118] and the effects of recuperator channel geometries [119] are available from the literature. Yilmaz et al. [103] presented the literature on optimisation based on entropy generation numbers, for the following heat exchangers: balanced and unbalanced counterflow heat exchangers, cross-flow heat exchangers, external flow heat exchange (like fins), two-phase flow heat exchangers, regenerative heat exchangers, plate-type heat exchangers and shell-and-tube heat exchangers. Heat exchangers with a liquid can be modelled with the help of references [1, 8, 103, 106, 108, 120–122]. Such heat exchangers can be found in applications such as exhaust gas heat recovery or intercooling.

Various attempts have been made at entropy generation minimisation for a specific component or a specific entropy generation mechanism, by defining the entropy generation equation as a function of geometry variables [1,8,120–122]. Eq. (24) for the recuperator or heat exchanger entropy generation rate in a solar thermal Brayton cycle can be geometrised similarly using the literature above.

Using the abovementioned literature, the authors recommend that Eq. (24) be geometrised (written in terms of recuperator geometry) for a specific heat exchanger design, so that geometry variables can be used in an objective function such as Eqs. (5)–(7).

3.3.3. Compressor and turbine

Eqs. (27) and (28) show the equations for the entropy generation rates for the compressor and turbine in the case of an ideal gas. These equations were also given by Jubeh [11] and Bejan [8]. Eqs. (27) and (28) are formulated in terms of the pressures and temperatures, which could be described by the isentropic efficiencies. The definitions of these efficiencies are commonly available from Weston [123], Dixon [124] and Haugwitz [109] for example. The geometries of compressors and turbines are often complex and the authors of this paper do not recommend that the entropy generation rate of the compressor and turbine be written in terms of geometry variables of the turbine or compressor. The calculation of entropy generation rate for these components at different temperatures and pressures is however important in the

derivation of the objective function. The pressures and temperatures can rather be written in terms of the geometry variables of other components

$$\dot{S}_{gen,c} = \dot{m}c_{p0i-e}\ln(T_e/T_i) - \dot{m}R\ln(P_e/P_i) + \frac{\dot{Q}_{loss,c}}{T_b} \tag{27}$$

$$\dot{S}_{gen,t} = \dot{m}c_{p0i-e}\ln(T_e/T_i) - \dot{m}R\ln(P_e/P)_i + \frac{\dot{Q}_{loss,t}}{T_b} \tag{28}$$

In this paper, the modelling of radial flow turbines is discussed in more detail since it is mostly used in small-scale power cycles.

3.3.3.1. Compressor. The compressor entropy generation rate can be calculated with Eq. (27). The compressor pressure ratio, mass flow rate and isentropic efficiencies are shown in a compressor map, given by the compressor manufacturer. These maps are mostly fitted with functions to make the modelling easier as shown by Haugwitz [109] and Frei [125], or fitted using software such as GTPower or TCMAP or as shown by Westin [126]. Methods to model the compressor based on its geometry are also available [127]. Wahlström and Eriksson [128] also presented methods of compressor modelling.

Haugwitz [109] presented a method by Gustafsson [129] wherein continuous ellipsoid curves were fitted to speed curves on the compressor map. According to Haugwitz [109], the parameters in the ellipsoid equation

$$\left(\frac{x}{a}\right)^z + \left(\frac{y}{b}\right)^z = c \tag{29}$$

can be adjusted to fit any speed curve on a typical compressor map. For parameterisation, the compressor efficiency map can be modelled as parabolic degradation curves [129]. The amount of degradation or curvature (d) is fitted based on data to get parameterisation for all speeds. According to Gustafsson [129] the following equation is valid for one speed [109]:

$$\eta_c = \eta_{c,\max} - d(\dot{m} - \dot{m}_{\max\ eff})^2 \tag{30}$$

where $\eta_{c,\max}$ is the maximum efficiency at that speed and $\dot{m}_{\max\ eff}$ is the corresponding mass flow for this maximum efficiency. Other compressor modelling options are described in the literature by various authors [126,130–133].

3.3.3.2. Turbine. Turbine maps are not as available as compressor maps and even if they are available, the turbine efficiency is not always shown on the map, but rather, a maximum efficiency is given. This often makes turbine modelling difficult. According to Watson and Janota [134] and experimental results by Westin [126], Haugwitz [109] and Zhuge et al. [127], it can be assumed that the turbine efficiency is a function of the pressure ratio and the speed of the shaft and that a maximum efficiency exists for each speed line. According to Reuter et al. [135], the instantaneous isentropic turbine efficiency can be calculated with

$$\eta_t(t) = \eta_m(t)\eta_{t,s} = \frac{\dot{W}_c(t) + \dot{W}_{acc}(t)}{\dot{W}_{t,s}(t)} \tag{31}$$

where $\dot{W}_{t,s}(t)$ is the instantaneous isentropic turbine power and the acceleration power can be determined with Reuter et al. [135] and Westin [126] as

$$\dot{W}_{acc}(t) = \left(\frac{2\pi}{60}\right)^2 J_{rotor} N_{rotor}(t)\frac{dN_{rotor}(t)}{dt} \tag{32}$$

Westin [126] suggested that the polar moment of inertia can be determined with the trifilar method as

$$J = \left(\frac{\tau}{2\pi}\right)^2 \frac{mgr^2}{l} \tag{33}$$

By assuming that the net power output (generator output power) would be equal to the acceleration power at no load, it can be shown that

$$\dot{m}c_pT_7\eta_t(1 - r_t^{(k-1)/k}) - \frac{1}{\eta_c}\dot{m}c_pT_1(r_c^{(k-1)/k} - 1) = \left(\frac{2\pi}{60}\right)^2 J_{rotor}N_{rotor}(t)\frac{dN_{rotor}(t)}{dt} \tag{34}$$

This equation can be used to determine the turbine efficiency if J is available and if a time dependant modelling is used. Another method to determine turbine efficiency, using the blade speed ratio, is discussed in the following paragraph.

According to Westin [126], Renberg [136], Watson and Janota [134] and Moraal and Kolmanovsky [131], steady flow theory states that if the data in an original turbine map, showing a curve on axes of pressure ratio vs. mass flow rate, is plotted as efficiency vs. blade speed ratio (U/C_s or BSR) all data points would fall onto a parabolic curve, with a definite peak. This peak should be positioned at $U/C_s = 0.707$ if the ratio of expansion between turbine rotor and housing (reaction) is 50% which seems to be common for vaneless radial turbines. This is also found in the doctoral thesis of Shaaban [137] who suggested that the blade speed ratio is the most commonly used parameter to define the turbine efficiency. This phenomenon seen when plotting efficiency vs. BSR is also found and shown by turbocharger testing and research [138]. It is debatable how the turbine works under unsteady flow—Westin [126] showed that the blade speed ratio at maximum efficiency could stay away from the standard value of 0.707, at non-steady conditions. According to Watson and Janota [134] the problem can be treated as quasi-steady flow, meaning that the turbine performs under non-steady flow in the same way as it would if those sudden flow conditions were steady. Evidence on the error introduced by this assumption is not entirely consistent and it is commonly believed that the error will not exceed 5% [134]. Capobianco and Marelli [139] showed that the errors are due to this assumption. The blade speed ratio can be determined as [126,128,132]

$$BSR = \frac{\frac{2\pi N}{60}\left(\frac{D}{2}\right)}{[2h_i(1 - r_t^{(1-k)/k})]^{1/2}} \tag{35}$$

so that when it is assumed that the maximum efficiency is found at $BSR = 0.707$, r_t can be found for a specific speed (N). The points of maximum turbine efficiency for each speed line can be plotted on the given turbine map (mass flow rate vs. pressure ratio). This maximum efficiency is also given on the turbine map. When considering experimental results by [109,126,127] it is assumed that the turbine efficiency can be presented, with pressure ratio on the x-axis, by plotting curves for each speed line which goes through the point of maximum efficiency. The efficiency can be modelled as a parabolic function of the blade speed ratio [125, 127, 128, 140]

$$\eta_t = \eta_{t,\max}\left(1 - \left(\frac{BSR - 0.6}{0.6}\right)^2\right) \tag{36}$$

According to Guzzella and Onder [133], simplified closed-form descriptions of the turbine's efficiency can be approximated by

$$\eta_t(BSR) = \eta_{t,\max}\left(\frac{2BSR}{BSR_{opt}} - \left(\frac{BSR}{BSR_{opt}}\right)^2\right) \tag{37}$$

where, in automotive applications, typical values are $\eta_{t,max} \approx 0.65$–$0.75$ and $BSR_{opt} \approx 0.55$–0.65. Thus, Eqs. (36) and (37) are essentially the same.

From the above it is concluded that from a basic turbine map the turbine efficiency can be calculated as a function of pressure ratio and speed with the use of the blade speed ratio. The authors

of this paper propose that this method will aid the analyst to a great extent in determining the entropy generation rate of the turbine.

3.3.4. Radiator

The radiator is used at the cold side of a closed solar thermal Brayton cycle. The entropy generation rate depends on the type of heat exchanger used for the radiator. Eq. (38) is given for the radiator if fins are used to cool down the working fluid (being an ideal gas) with a natural external flow (being air)

$$\dot{S}_{gen} = \frac{\dot{Q}_B}{T_B} + \dot{m}c_{p0} \ln\left(\frac{T_e}{T_i}\right) - \dot{m}R \ln\left(\frac{P_e}{P_i}\right) \tag{38}$$

where the subscript, B, refers to the base where the fins are attached. According to Bejan [8], Eq. (38) can also be written as

$$\dot{S}_{gen} = N\left[\frac{\dot{Q}_{B,sngl}(T_B - T_\infty)}{T_\infty^2} + \frac{F_D V_\infty}{T_\infty}\right] + \dot{m}c_{p0} \ln\left(\frac{T_e}{T_i}\right) - \dot{m}R \ln\left(\frac{P_e}{P_i}\right) \tag{39}$$

where it is assumed that $\dot{Q}_{loss,radiator} = \dot{Q}_B = N\dot{Q}_{B,sngl}$ and N is the number of fins.

There is competitiveness between heat transfer and fluid mechanics terms to get an optimal radiator size with minimum entropy generation [1,8,17].

3.3.5. Other entropy generation mechanisms

Other entropy generation mechanisms occurring in the solar thermal Brayton cycle include entropy generation due to mixing (refer to [8]), filters, pipes, pipe bends and storage. The entropy generation due to these mechanisms when assuming an ideal gas flow can be calculated with

$$\dot{S}_{gen} = \frac{\dot{Q}_{loss}}{T_b} + \dot{m}c_{p0} \ln\left(\frac{T_e}{T_i}\right) - \dot{m}R \ln\left(\frac{P_e}{P_i}\right) \tag{40}$$

The modelling of fluid flow in straight pipes, bent pipes and flow splits is discussed in the literature [109,136]. Other typical flow restrictions can be modelled as shown by Frei [125]. Phase change material has been modelled by Wu et al. [141].

Often, the bearings of turbo-machines are cooled using oil or water. The entropy generated from such a system can be described as shown in Eq. (41) and included in an objective function. The cooling flow loop can also be modelled separately or as the heat loss in Eqs. (27) and (28).

$$\dot{S}_{gen} = \frac{\dot{Q}_{loss}}{T_b} \tag{41}$$

When a solid or a liquid crosses the control volume boundary of the system, the entropy change can be modelled with Eq. (42) instead of Eq. (4)

$$s_e - s_i = c \ln \frac{T_e}{T_i} \tag{42}$$

4. Conclusions and recommendations

In this paper, new perspectives, conflicts and recommendations were highlighted regarding the derivation of an objective function which includes various geometries from different components of a solar thermal Brayton cycle. Optimisation studies of the Brayton cycle as relevant to the solar thermal Brayton cycle were reviewed. The influencing factors to optimisation were identified. The method of total entropy generation minimisation was highlighted as it allows heat transfer and fluid flow terms to be available for optimisation in a single equation, so that geometry variables of different components of a solar thermal Brayton cycle can be optimised simultaneously. The importance of the second law of thermodynamics, including geometry into optimisation and the importance of the selection of the control volume boundary, was emphasised. The modelling of various components to construct an objective function for optimisation was discussed. Such an equation can be applied for example to optimise the component geometries in a steady-state solar thermal Brayton cycle such that the system produces maximum net power output.

Various studies have stressed the significance of the optimisation of the global performance of a system, by minimising the sum of the irreversibilities from all the different components or processes of the system (distributing the entropy generation rate through the system by optimally sizing the hardware, instead of optimising components independently) [1,17,18,38,108,121,122]. For future work it is recommended that geometry optimisation studies be done on especially intercoolers and reheaters (a second solar receiver) in the solar thermal Brayton cycle, as the inclusion of these components can largely increase the efficiency of such a system. The authors also recommend that constraints on the objective function, such as component size, cost and weight, should be incorporated depending on the component types chosen in an analysis.

In this paper it was shown that from a basic turbine map, turbine efficiency can be calculated as a function of pressure ratio and speed with the use of the blade speed ratio. It is proposed that this method will aid the analyst to a great extent in modelling and determining the entropy generation rate of the turbine in the solar thermal Brayton cycle. The inclusion of turbine and compressor geometry variables for optimisation in the objective function can be considered for future work. The authors referred to different types of receivers and heat exchangers in this paper and recommend that these components can be modelled and optimised in terms of total system entropy generation minimisation for comparison purposes. Entropy generation in the transient state was not shown in this study and can be recommended for future work. Other entropy generation mechanisms in the solar thermal Brayton cycle, not mentioned in this paper, and the modelling thereof can also be recommended for future work.

The work in this paper is applicable to solar thermal studies in general but focused mainly on the small-scale solar thermal Brayton cycle. With this paper, the authors hope to contribute in making solar thermal Brayton systems successful and applicable in future power generation.

Acknowledgement

This work is based on the research supported by the National Research Foundation (NRF), University of Pretoria, CRSES, the Solar Hub between the University of Pretoria and Stellenbosch University, TESP, NAC, EEDSH Hub, Energy-IRT and the CSIR. The financial assistance of the National Research Foundation (NRF) towards this research is hereby acknowledged. Opinions expressed and conclusions arrived at are those of the author and are not necessarily to be attributed to the NRF.

References

[1] Bejan A, Tsatsaronis G, Moran M. Thermal design and optimization. New York: John Wiley & Sons, Inc; 1996.
[2] Chen L, Zhang W, Sun F. Power, efficiency, entropy-generation rate and ecological optimization for a class of generalized irreversible universal heat-engine cycles. Applied Energy 2007;84:512–25.
[3] Mills D. Advances in solar thermal electricity technology. Solar Energy 2004;76:9–31.
[4] Stine BS, Harrigan RW. Solar energy fundamentals and design. New York: John Wiley & Sons, Inc.; 1985.
[5] Narendra S, Kaushik SC, Misra RD. Exergetic analysis of a solar thermal power system. Renewable Energy 2000;19:135–43.

[6] Duffie JA, Beckman WA. Solar engineering of thermal processes. New York: John Wiley & Sons, Inc.; 1991.
[7] Sonntag RE, Borgnakke C, Van Wylen GJ. Fundamentals of thermodynamics. New York: John Wiley & Sons, Inc.; 2003.
[8] Bejan A. Entropy generation through heat and fluid flow. Colorado: John Wiley & Sons, Inc.; 1982.
[9] Izquierdo M, De Vega M, Lecuona A, Rodríguez P. Compressors driven by thermal solar energy: entropy generated, exergy destroyed and exergetic efficiency. Solar Energy 2002;72(4):363–75.
[10] Barrett MJ, Reid BM. System mass variation and entropy generation in 100-kWe Closed-Brayton-Cycle Space Power Systems. Space Technology and Application International Forum STAIE 2004;699:445–52.
[11] Jubeh NM. Exergy analysis and second law efficiency of a regenerative Brayton cycle with isothermal heat addition. Entropy 2005;7(3):172–87.
[12] Bejan A. Fundamentals of exergy analysis, entropy generation minimization, and the generation of flow architecture. International Journal of Energy Research 2002;26:545–65, http://dx.doi.org/10.1002/er.804.
[13] Kalogirou SA. Solar thermal collectors and applications. Progress in Energy and Combustion Science 2004;30:231–95.
[14] Keenan JH. Availability and irreversibility in thermodynamics. British Journal of Applied Physics 1951;2:183–92.
[15] Bejan A. Theory of heat transfer-irreversible power plants. International Journal of Heat and Mass Transfer 1988;31(6):1211–9.
[16] Bejan A. The equivalence of maximum power and minimum entropy generation rate in the optimization of power plants. Journal of Energy Resources Technology 1996;118(2):98–101.
[17] Bejan A. Method of entropy generation minimization, or modelling and optimization based on combined heat transfer and thermodynamics. Revue Générale de Thermique 1996;35:637–46.
[18] Shiba T, Bejan A. Thermodynamic optimization of geometric structure in the counterflow heat exchanger for an environmental control system. Energy 2001;26:493–511.
[19] Torres-Reyes E, Navarrete-González JJ, Cervantes-de Gortari JG. Thermodynamic optimization as an effective tool to design solar heating systems. Energy 2004;29:2305–15.
[20] Chen L, Ni N, Wu C, Sun F. Performance analysis of a closed regenerated Brayton heat pump with internal irreversibilities. International Journal of Energy Research 1999;23:1039–50.
[21] Zheng S, Chen J, Sun F, Lin G. Performance characteristics of an irreversible solar-driven Braysson heat engine at maximum efficiency. Renewable Energy 2005;30:601–10.
[22] Wu L, Lin G, Chen J. Parametric optimization of a solar-driven Braysson heat engine with variable heat capacity of the working fluid and radiation–convection heat losses. Renewable Energy 2010;35:95–100.
[23] Salamon P, Hoffmann KH, Schubert S, Berry S, Andresen B. What conditions make minimum entropy production equivalent to maximum power production? Journal of Non-Equilibrium Thermodynamics 2001;26:73–83.
[24] Chen L, Sun F, Wu C, Kiang RL. Theoretical analysis of the performance of a regenerative closed Brayton cycle with internal irreversibilities. Energy Conversion and Management 1997;38(9):871–7.
[25] Wu C, Chen L, Sun F. Performance of a regenerative Brayton heat engine. Energy 1996;21(2):71–6.
[26] Stevens T, Verplaetsen F, Baelmans M. Requirements for recuperators in micro gas turbines. In: The fourth international workshop on micro and nanotechnology for power generation and energy conversion applications, Kyoto, Japan; 2004. p. 96–9.
[27] Stevens T, Baelmans M. Optimal pressure drop ratio for micro recuperators in small sized gas turbines. Applied Thermal Engineering 2008;28:2353–9.
[28] Riazi H, Ahmed NA. Effect of the ratio of specific heats on a small scale solar Brayton cycle. (*IEF-IEC2012*) *Procedia Engineering* 2012;49:263–70.
[29] Roco JMM, Velasco S, Medina A, Calvo Hernández A. Optimum performance of a regenerative Brayton thermal cycle. Journal of Applied Physics 1997;82(6):2735–41.
[30] Cheng C, Chen C. Maximum power of an endoreversible intercooled Brayton cycle. International Journal of Energy Research 2000;24:485–94.
[31] Wang W, Chen L, Sun F, Wu C. Power optimization of an endoreversible closed intercooled regenerated Brayton cycle. International Journal of Thermal Sciences 2005;44:89–94.
[32] Zhang Y, Lin B, Chen J. Optimum performance characteristics of an irreversible solar-driven Brayton heat engine at the maximum overall efficiency. Renewable Energy 2007;32:856–67.
[33] Le Roux WG, Bello-Ochende T, Meyer JP. Operating conditions of an open and direct solar thermal Brayton cycle with optimised cavity receiver and recuperator. Energy 2011;36:6027–36.
[34] Le Roux WG, Bello-Ochende T, Meyer JP. Thermodynamic optimisation of an integrated design of a small-scale solar thermal Brayton cycle. International Journal of Energy Research 2012;36:1088–104.
[35] Le Roux WG, Bello-Ochende T, Meyer JP. Optimum performance of the small-scale open and direct solar thermal Brayton cycle at various environmental conditions and constraints. Energy 2012;46:42–50.
[36] Karsli S. Performance analysis of new-design solar air collectors for drying applications. Renewable Energy 2007;32:1645–60.
[37] Gomez A, Azzaro-Pantel C, Domenech S, Pibouleau L, Latgé C, Haubensack D, et al. Exergy analysis for generation IV nuclear plant optimization. International Journal of Energy Research 2010;34:609–25, http://dx.doi.org/10.1002/er.1575.
[38] Bejan A. Advanced engineering thermodynamics. second ed.. Durham: John Wiley & Sons, Inc.; 1997.
[39] Cervantes JG, Torres-Reyes E. Experiments on a solar-assisted heat pump and an exergy analysis of the system. Applied Thermal Engineering 2002;22:1289–97.
[40] Amhalhel GA, Furmański P. Exergy analysis of different design concepts of receivers/reactors for thermochemical conversion of concentrated solar energy, vols. 89/90. Institute of Heat Engineering; 2004.
[41] Sieniutycz S, Kuran P. Nonlinear models for mechanical energy production in imperfect generators driven by thermal or solar energy. International Journal of Heat and Mass Transfer 2005;48:719–30.
[42] Hepbasli A. A key review on exergetic analysis and assessment of renewable energy resources for a sustainable future. Renewable and Sustainable Energy Reviews 2008;12:593–661.
[43] Lampinen MJ, Wikstén R. Theory of effective heat-absorbing and heat-emitting temperatures in entropy and exergy analysis with applications to flow systems and combustion processes. Journal of Non-Equilibrium Thermodynamics 2006;31(3):257–91, http://dx.doi.org/10.1515/JNETDY.2006.012.
[44] Bejan A. Entropy generation minimization. CRC Press; 1996.
[45] Tolman RC, Fine PC. On the irreversibility production of entropy. Reviews of Modern Physics 1948;10:51–77.
[46] Holmberg H, Ruohonen P, Ahtila P. Determination of the real loss of power for a condensing and a backpressure turbine by means of second law analysis. Entropy 2009;11:702–12, http://dx.doi.org/10.3390/e11040702.
[47] Izquierdo Millan M, Hernandez F, Martin E. Available solar exergy in an absorption cooling process. Solar Energy 1996;56(6):505–11.
[48] Petela R. Engineering thermodynamics of thermal radiation. New York: McGraw-Hill; 2010.
[49] Joshi AS, Dincer I, Reddy BV. Development of new solar exergy maps. International Journal of Energy Research 2009;33:709–18.
[50] Onyegegbu SO, Morhenne J. Transient multidimensional second law analysis of solar collectors subjected to time-varying insolation with diffuse components. Solar Energy 1993;50(1):85.
[51] Agudelo A, Cortés C. Thermal radiation and the second law. Energy 2010;35:679–91.
[52] Chu SX, Liu LH. Analysis of terrestrial solar radiation exergy. Solar Energy 2009;83:1390–404.
[53] Zamfirescu C, Dincer I. How much exergy one can obtain from incident solar radiation? Journal of Applied Physics 2009:105.
[54] Wright SE, Rosen MA. Exergetic efficiencies and the exergy content of terrestrial solar radiation. Journal of Solar Energy Engineering 2004;126:673–6.
[55] Petela R. Exergy of undiluted thermal radiation. Solar Energy 2003;74:469–88.
[56] Bejan A. Unification of three different theories concerning the ideal conversion of enclosed radiation. Transactions of the ASME 1987;109:46.
[57] Reddy RS, Kaushik SC, Tyagi SK. Exergetic analysis and performance evaluation of parabolic trough concentrating solar thermal power plant (PTCSTPP). Energy 2012;39:258–73.
[58] Farahat S, Sarhaddi F, Ajam H. Exergetic optimization of flat plate solar collectors. Renewable Energy 2009;34:1169–74.
[59] Moynihan PI. Second-law efficiency of solar-thermal cavity receivers. Report no. JPL 83-97; 1983. Pasadena, CA: Jet Propulsion Laboratory.
[60] Torchia-Nunez JC, Porta-Gandara MA, Cervantes-de Gortari JG. Exergy analysis of a passive solar still. Renewable Energy 2008;33:608–16.
[61] Petela R. Exergy of heat radiation. ASME Journal of Heat Transfer 1964;86:187–92.
[62] Eskin N. Transient performance analysis of cylindrical parabolic concentrating collectors and comparison with experimental results. Energy Conversion & Management 1999;40:175–91.
[63] Landsberg PT, Tonge G. Thermodynamics of the conversion of diluted radiation. Journal of Physics A: Mathematical and General 1979;12:551.
[64] Kalogirou SA. Entropy generation minimization of imaging concentrating solar collectors. In: ISES 2003 solar world congress, Goteborg, Sweden; 2003.
[65] Hu Y, Schaefer LA, Hartkopf V. Detailed energy and exergy analysis for a solar lithium bromide absorption chiller and a conventional electric chiller (R134a). In: Proceedings of the ASME 2011 international mechanical engineering congress & exposition; 2011. IMECE2011-64266.
[66] Li. Y, He Y, Wang Z, Xu C, Wang W. Exergy analysis of two phase change materials storage system for solar thermal power with finite-time thermodynamics. Renewable Energy 2012;39:447–54.
[67] Xu C, Wang Z, Li X, Sun F. Energy and exergy analysis of solar power tower plants. Applied Thermal Engineering 2011;31:3904–13.
[68] Bejan A, Kearney DW, Kreith F. Second law analysis and synthesis of solar collector systems. Journal of Solar Energy Engineering 1981;103:23–8.
[69] Bejan A. Extraction of exergy from solar collectors under time-varying conditions. International Journal of Heat and Fluid Flow 1982;3(2):67–72.
[70] Ozturk M. In: Kei Eguchi, editor, Clean energy systems and experiences: exergy analysis of low and high temperature water gas shift reactor with parabolic concentrating collector; 2010. Sciyo: Croatia.
[71] Najian MR. Exergy analysis of flat plate solar collector. MS thesis. Tehran, Iran: Department of Mechanical Engineering, College of Engineering, Tehran University; 2000.
[72] Torres-Reyes E, Cervantes de Gortari JG, Ibarra-Salazar BA, Picon-Nunez M. A design method of flat-plate solar collectors based on minimum entropy generation. Exergy 2001;1(1):46–52.
[73] Wong LT, Chow WK. Solar radiation model. Applied Energy 2001;69:91–224.

[74] Remund J, Kunz S, Lang, R. METEONORM: Global meteorological database for solar energy and applied climatology; 1999. Available at: http://www.meteotest.ch, www.meteonorm.com.
[75] You Y, Hu EJ. A medium-temperature solar thermal power system and its efficiency optimisation. Applied Thermal Engineering 2002;22:357–64.
[76] Agrawal DC. Solar luminous constant versus lunar luminous constant. Latin-American Journal of Physics Education 2010;4(2):325–8.
[77] De Vos A. Endoreversible thermodynamics of solar energy conversion. New York: Oxford University Press; 1992.
[78] Pridasawas W, Lundqvist P. An exergy analysis of a solar-driven ejector refrigeration system. Solar Energy 2004;76:369–79.
[79] Winter CJ, Sizmann RL, Vant-Hull LL. Solar power plants. New York: Springer; 1991.
[80] Rayegan R, Tao YX. A procedure to select working fluids for Solar Organic Rankine Cycles (ORCs). Renewable Energy 2011;36:659–70.
[81] Torres-Reyes E, Ibarra-Salazar BA, Cervantes-De GJG. Thermoeconomic analysis at optimal performance of non-isothermal flat-plate solar collectors. International Journal of Applied Thermodynamics 2001;4(2):103–9 (ISSN1301-9724).
[82] Bode SJ, Gauché P. Review of optical software for use in concentrated solar power systems. SASEC 2012; 21–23 May 2012. Stellenbosch, South Africa.
[83] Bertocchi R, Karni J, Kribus A. Experimental evaluation of a non-isothermal high temperature solar particle receiver. Energy 2004;29:687–700.
[84] Kim K, Siegel N, Kolb G, Rangaswamy V, Moujaes SF. A study of solid particle flow characterization in solar particle receiver. Solar Energy 2009;83:1784–93.
[85] Miller F, Koenigsdorff R. Theoretical analysis of a high-temperature small-particle solar receiver. Solar Energy Materials 1991;24:210–21.
[86] Heller P, Pfänder M, Denk T, Tellez F, Valverde A, Fernandez J, et al. Test and evaluation of a solar powered gas turbine system. Solar Energy 2006;80:1225–30.
[87] Hischier I, Hess D, Lipiński W, Modest M, Steinfeld A. Heat transfer analysis of a novel pressurized air receiver for concentrated solar power via combined cycles. Journal of Thermal Science and Engineering Applications 2009041002.
[88] Garcia RF, Formoso RB Catoira AD, Gomez JR. Pressurized concentrated solar power receiver designed to operate with closed Brayton cycles. In: International conference on renewable energies and power quality (ICREPQ'12), Santiago de Compostela, Spain; 2012.
[89] Kretzschmar H, Gauché P. Hybrid pressurized air receiver for the SUNSPOT cycle. SASEC 2012; 21–23 May 2012. Stellenbosch, South Africa.
[90] Ávila-Marín AL. Volumetric receivers in solar thermal power plants with central receiver system technology: a review. Solar Energy 2011;85:891–910.
[91] Karni J, Kribus A, Rubin R, Doron P. The Porcupine: a novel high-flux absorber for volumetric solar receivers. Journal of Solar Energy Engineering 1998;120:85–95.
[92] Shuai Y, Xia X, Tan H. Radiation performance of dish solar concentrator/cavity receiver systems. Solar Energy 2008;82:13–21.
[93] Harris JA, Lenz TG. Thermal performance of solar concentrator/cavity receiver systems. Solar Energy 1985;34(2):135–42.
[94] Steinfeld A, Schubnell M. Optimum aperture size and operating temperature of a solar cavity-receiver. Solar Energy 1993;50(1):19–25.
[95] Prakash M, Kedare SB, Nayak JK. Investigations on heat losses from a solar cavity receiver. Solar Energy 2009;83:157–70.
[96] Sendhil Kumar N, Reddy KS. Comparison of receivers for solar dish collector system. Energy Conversion and Management 2008;49:812–9.
[97] Sendhil Kumar N, Reddy KS. Numerical investigation of natural convection heat loss in modified cavity receiver for fuzzy focal solar dish concentrator. Solar Energy 2007;81:846–55.
[98] Reddy KS, Sendhil Kumar N. An improved model for natural convection heat loss from modified cavity receiver of solar dish concentrator. Solar Energy 2009;83:1884–92.
[99] Reddy KS, Sendhil Kumar N. Combined laminar natural convection and surface radiation heat transfer in a modified cavity receiver of solar parabolic dish. International Journal of Thermal Sciences 2008;47:1647–57.
[100] Ishikawa H, Hobson PA. Optimisation of heat exchanger design in a thermo-acoustic engine using a second law analysis. International Communications in Heat and Mass Transfer 1996;23(3):325–34.
[101] Lerou PPPM, Veenstra TT, Burger JF, Ter Brake HJM, Rogalla H. Optimization of counterflow heat exchanger geometry through minimization of entropy generation. Cryogenics 2005;45:659–69.
[102] Oğulata RT, Doba F, Yilmaz T. Irreversibility analysis of cross flow heat exchangers. Energy Conversion and Management 2000;41(15):1585–99.
[103] Yilmaz M, Sara ON, Karsli S. Performance evaluation criteria for heat exchangers based on second law analysis. *Exergy: An International Journal* 2001;1(4):278–94.
[104] Sarangi S, Chowdhury K. On the generation of entropy in a counterflow heat exchanger. Cryogenics 1982;22(2):63–5.
[105] Cornelissen RL, Hirs GG. Exergetic optimization of a heat exchanger. Energy Conversion and Management 1997;1(15–17):1567–76.
[106] Zimparov V. Extended performance evaluation criteria for enhanced heat transfer surfaces: heat transfer through ducts with constant heat flux. International Journal of Heat and Mass Transfer 2001;44(1):169–80.
[107] Hesselgreaves JE. Rationalisation of second law analysis of heat exchangers. International Journal of Heat and Mass Transfer 2000;43(22):4189–204.
[108] Ordóñez JC, Bejan A. Entropy generation minimization in parallel-plates counterflow heat exchangers. International Journal of Energy Research 2000;24:843–64.
[109] Haugwitz S. Modelling of microturbine systems. Master thesis. Department of Automatic Control, Lund Institute of Technology; 2002. ISSN 0280-5316, ISRN LUTFD2/TFRT-5687-SE.
[110] Kreith F, Kreider JF. Principles of solar engineering. Colorado: Hemisphere; 1978.
[111] Shah RK. Compact heat exchangers for micro-turbines. In: Micro gas turbines. Educational notes RTO-EN-AVT-131. Paper 2; 2005. p. 2-1–18. Neuilly-sur-Seine, France: RTO. Available from: 〈http://www.rto.nato.int/abstracts.asp〉.
[112] McDonald CF. Low-cost compact primary surface recuperator concept for microturbines. Applied Thermal Engineering 2000;20:471–97.
[113] McDonald CF. Recuperator considerations for future higher efficiency micro-turbines. Applied Thermal Engineering 2003;23:1463–87.
[114] Pra F, Tochona P, Mauget C, Fokkens J, Willemsen S. Promising designs of compact heat exchangers for modular HTRs using the Brayton cycle. Nuclear Engineering and Design 2008;238:3160–73.
[115] Tsai B, Wang YL. A novel Swiss–Roll recuperator for the microturbine engine. Applied Thermal Engineering 2009;29:216–23.
[116] Traverso A, Massardo AF. Optimal design of compact recuperators for microturbine application. Applied Thermal Engineering 2005;25:2054–71.
[117] Ultiainen E, Sundén B. Evaluation of the cross corrugated and some other candidate heat transfer surfaces for microturbine recuperators. Transactions of the ASME 2002;124:550–60.
[118] Rogiers F, Stevens T, Baelmans M. Optimal recuperator design for use in a micro gas turbine. In: The sixth international workshop on micro and nanotechnology for power generation and energy conversion applications; November 29–December 1, 2006, Berkeley, USA. p. 133–6.
[119] Burrow BV. The effect of recuperator geometry on a regenerated Brayton cycle. Thesis. Monterey: United States Naval Postgraduate School; 1969.
[120] Ratts BE, Raut AG. Entropy generation minimization of fully developed internal flow with constant heat flux. Journal of Heat Transfer 2004;126(4):656–9.
[121] Zimparov VD, Da Silva AK, Bejan A. Thermodynamic optimization of tree-shaped flow geometries with constant channel wall temperature. International Journal of Heat and Mass Transfer 2006;49:4839–49.
[122] Zimparov VD, Da Silva AK, Bejan A. Thermodynamic optimization of tree-shaped flow geometries. International Journal of Heat and Mass Transfer 2006;49:1619–30.
[123] Weston KC. Energy conversion; 2000. Tulsa: Brooks/Cole [e-book]. Available at: 〈http://www.personal.utulsa.edu/~kenneth-weston/〉.
[124] Dixon SL. Fluid mechanics and thermodynamics of turbomachinery. fifth ed.. Liverpool: Elsevier Butterworth-Heinemann; 2005.
[125] Frei SA. Performance and drivability optimization of turbocharged engine systems. A dissertation submitted to the Swiss Federal Institute of Technology, Zurich, for the degree of Doctor of Technical Sciences; 2004.
[126] Westin F. Simulation of turbocharged SI-engines—with focus on the turbine. Doctoral thesis. KTH School of Industrial Engineering and Management, TRITA—MMK 2005:05. Stockholm: Royal Institute of Technology; 2005.
[127] Zhuge W, Zhang Y, Zheng X, Yang M, He Y. Development of an advanced turbocharger simulation method for cycle simulation of turbocharged internal combustion engines. *Proceedings of the Institution of Mechanical Engineers, Part D*: *Journal of Automobile Engineering* 2009;223:661, http://dx.doi.org/10.1243/09544070JAUTO975.
[128] Wahlström J, Eriksson L. Modeling diesel engines with a variable-geometry turbocharger and exhaust gas recirculation by optimization of model parameters for capturing non-linear system dynamics. Proceedings of the Institution of Mechanical Engineers, Part D, Journal of Automobile Engineering 2011;*225*(*July (7)*).
[129] Gustafsson J. Static and dynamic modelling of gas turbine in advanced cycles. Technical report licentiate thesis. Lund Institute of Technology, Lund, Sweden; 1998.
[130] Leufvén O. Compressor modeling for control of automotive two stage turbochargers. Thesis no. 1463. Linköpings universitet, Department of Electrical Engineering, Linköping, Sweden; 2010.
[131] Moraal P, Kolmanovsky I. Turbocharger modeling for automotive control applications. In: International congress and exposition, Detroit, MI; March 1–4, 1999.
[132] Batteh JJ, Newman CE. Detailed simulation of turbocharged engines with modelica; March 3 and 4, 2008. The Modelica Association.
[133] Guzzella L, Onder CH. Introduction to modeling and control of internal combustion engine systems. second ed.. Berlin, Germany: Springer-Verlag; http://dx.doi.org/10.1007/978-3-642-10775-7.
[134] Watson N, Janota M. Turbocharging the internal combustion engine. Hong Kong: The Mechanical Press Ltd; 1982.
[135] Reuter S, Koch A, Kaufmann A. Extension of performance maps of radial turbocharger turbines using pulsating hot gas flow. 9th International Conference on Turbocharging and Turbochargers, London. Institution of Mechanical Engineers 2010:262–80.
[136] Renberg U. 1D engine simulation of a turbocharged SI engine with CFD computation on components. Licentiate thesis. Stockholm: Department of Machine Design, Royal Institute of Technology; 2008. S-100 44. ISSN 1400-1179.

[137] Shaaban S. Experimental investigation and extended simulation of turbocharger non-adiabatic performance. Doctoral thesis. Hannover; 2004.
[138] Newton P, Copeland C, Martinez-Botas R, Seiler M. An audit of aerodynamic loss in a double entry turbine under full and partial admission. International Journal of Heat and Fluid Flow 2012;33:70–80.
[139] Capobianco M, Marelli S. Experimental analysis of unsteady flow performance in an automotive turbocharger turbine fitted with a waste-gate valve. In: Proceedings of the IMechE. Part D: Journal of Automobile Engineering, vol. 225; 2011.
[140] Jung M, Ford RG, Glover K, Collings N, Christen U, Watts MJ. Parameterization and transient validation of a variable geometry turbocharger for mean-value modeling at low and medium speed-load points; 2002. Society of Automotive Engineers, Inc. Paper 2002-01-2729.
[141] Wu Y, Ren J, Gu Z, Ma C. Dynamic simulation of closed Brayton cycle solar thermal power system. In: SET2004—third international conference on sustainable energy technologies, Nottingham, UK; 28–30 June 2004.